www.czasopisma.pan.pl PAN POLSKA AKADEMIA NAUK www.journals.pan.pl

A R C H I V E S O F M E T A L L U R G Y A N D M A T E R I A L S

Volume 58 2013 Issue 2

DOI: 10.2478/amm-2013-0015

W. MAZIARZ*, P. CZAJA*, T. CZEPPE*, A. GÓRAL*, L. LITYŃSKA-DOBRZYŃSKA*, Ł. MAJOR*, J. DUTKIEWICZ*

STRUCTURE AND MARTENSITIC TRANSFORMATION IN $Ni_{44}Mn_{43.5}Sn_{12.5-x}Al_x$ HEUSLER ALLOYS

ANALIZA STRUKTURY I PRZEMIANY MARTENZYTYCZNEJ W STOPACH HEUSLERA $Ni_{44}Mn_{43.5}Sn_{12.5-x}Al_x$

Alloys with constant Ni/Mn ratio equal to 1.01 of nominal compositions $Ni_{44}Mn_{43.5}Sn_{12.5-x}Al_x$ (x = 0, 1, 2 and 3) were induction cast, homogenized in vacuum for 6 hours at 1000°C, annealed for 1 h at 900 and water quenched for solution treatment (ST). Differential scanning calorimetry (DSC) studies revealed that the quenched alloys undergo martensitic transformation with martensite start temperatures (M_s) ranging from – 140 up to – 80°C. An increase of M_s temperature with increasing of the aluminum content as well as the linear relationship between M_s and the conductive electron concentration (e/a) was observed. DSC has been used also to estimate the associated entropy change from the transformation heat Q and peak position temperature Tp; corresponding to $\Delta S \approx Q/Tp$. X-Ray diffraction phase analyses performed at room temperature proved that in all ST alloys the $L2_1$ Heusler structure is present. However, a different degree of order of this phase was observed, what was manifested by a decrease of intensity of the 111 superlattice reflection of the $L2_1$ structure with an increase of Al content. The ordering behavior was also proven by the transmission electron microscopy (TEM) investigations, particularly electron diffraction patterns. The evolution of microstructure after different treatments was also illustrated by light microscopy observations.

Keywords: magnetic shape memory, NiMnSnAl alloys, martensitic transition, ordering of parent phase

Stopy o stałym stosunku Ni/Mn wynoszącym 1,01 i o składzie $Ni_{44}Mn_{43.5}Sn_{12.5-x}Al_x$ (x= 0, 1, 2, 3) odlewano w piecu indukcyjnym a następnie poddano wyżarzaniu w próżni w temperaturze 1000°C przez 6 godzin oraz obróbce cieplnej polegającej na wygrzaniu w temperaturze 900°C przez okres 1 h i przesyceniu poprzez szybkie chłodzenie w wodzie o temperaturze pokojowej. Wyniki uzyskane przy użyciu różnicowej kalorymetrii skaningowej wykazały, że przesycone stopy ulegają przemianie martenzytycznej, której początek w zależności od składu stopu mieści się w zakresie – 140 do – 80°C. Stwierdzono, że wraz ze wzrostem zawartości aluminium w stopach rośnie temperatura początku przemiany martenzytycznej oraz, że zależność tej temperatury od wartości stężenia elektronów walencyjnych e/a ma charakter liniowy. Badania kalorymetryczne posłużyły również do oszacowania wielkości zmian entropii towarzyszącej przemianie fazowej do czego wykorzystano znajomość ilości ciepła Q przemiany a także pozycję piku temperaturowego zgodnie z zależnością Tp: $\Delta S \approx Q/Tp$. Analiza rentgenowska w temperaturze pokojowej wykazała, że wszystkie stopy po obróbce cieplnej stopy posiadają strukturę Henslera o uporządkowaniu typu $L2_1$. Jednakże, stopień uporządkowania tej struktury w zależności od zawartości Al w stopach jest różny na co wskazuje zanik refleksu {111}charakterystycznego dla nadstruktury $L2_1$ wraz ze wzrostem stężenia Al. Zmiany stopnia uporządkowania zostały potwierdzone przy pomocy transmisyjnej mikroskopii elektronowej a zwłaszcza dzięki dyfrakcji elektronowej. Zamiany mikrostruktury po różnych etapach wytwarzania i obróbki cieplne zilustrowano przy użyciu mikroskopii świetlnej.

1. Introduction

Ni-Mn-Sn – based Heusler alloys (HAs) have received considerable attention due to their unique properties such as the metamagnetic shape memory effect, the inverse magnetocaloric effect, the giant magnetoresistance effect and the giant magnetothermal conductivity [1]. Recently Chen et al. [2] have reported that replacement of Sn with Al in $Ni_{43}Mn_{46}Sn_{11-x}Al_x$ (x=0, 0.5, 1, 2) leads to a decrease of cell volume with increasing Al content what then results in the increase of the martensite start transition temperature (M_s). On the other hand M_s is well known to be sensitive to the value of valence electron concentration (e/a) [3]. It increases almost linearly with increasing electron density (decreasing the X element content in Ni-Mn-X based alloys X = Ga, Sn, In, Sb). Additionally, according to literature reports varying e/a ratio in case of Ni-Mn-Ga, Ni-Mn-In and Ni-Mn-Sn influences also the martensitic structure, as well as the enthalpy and entropy change, which both increase with increasing electron concentration [4]. Introducing a dopant and manipulating e/a are normally used to tune M_s. An alternative way to tune phase transformation temperature is through influencing the atomic ordering. For instance, it has been observed that M_s and metamagnetic behavior may sometimes disappear in an annealed state due to the kinetic arrest effect [5,6]. This is related to the fact that most of the shape memory alloys (SME) are β-phase alloys and as such they contain a high population of frozen in vacancies (in result of rapid quenching) and either the nearest

* INSTITUTE OF METALLURGY AND MATERIALS SCIENCE POLISH ACADEMY OF SCIENCES, 25 REYMONTA STR., 30-059 KRAKÓW, POLAND

neighbor (NN) atomic ordering or the next nearest neighbor atomic ordering (NNN) or both [7]. Furthermore some degree of chemical disorder linked to occupation of lattice sites is an intrinsic property of HAs. Fully ordered state ($L2_1$) in reality is hardly attainable. Therefore a different variations of disorder are possible (B2, DO_3, A2) [8]. These combined may exert a significant influence on M_s.

This paper describes how the Al substitution for Sn in $Ni_{44}Mn_{43.5}Al_xSn_{12.5-x}$ influences the ordering of phases present in the alloys and how it in turn affects the martensite start transition temperature M_s. It is interesting to note that although in this instance the valence electron concentration e/a decreases with increasing Al content the M_s temperature goes up, unlike in most of the Heusler alloys.

2. Experimental

Four alloys with nominal compositions of $Ni_{44}Mn_{43.5}Al_xSn_{12.5-x}$ (x= 0, 1, 2, 3 at. %), designated as 0Al, 1Al, 2Al, 3Al respectively, were prepared by induction melting under argon atmosphere using pure starting elements (<99.9%). The ingots of 15 mm diameter were cut into small pieces and then homogenized in vacuum for 6 hours at 1000°C. Next, they were encapsulated into the quartz tube under argon atmosphere and solution treated (ST) at 900°C for 1h and water quenched (WQ). The Leica DM IRM light microscope (LM) was used for microstructure observation of as homogenized as well as ST alloys. The phase analysis of ST alloys was performed using a Philips (PW1830) diffractometer with Co K_α radiation (λ =1.78896 Å). Differential scanning calorimeter (DSC) TA Q1000 was used for determination of characteristic temperatures of martensitic transformation during cooling and heating cycles at 10°C/min rate. The ordering process of ST alloys was analyzed by using transmission electron microscope (TEM) Tecnai G2. The thin foils for TEM observation were prepared by dimpling followed by ion milling methods. The thin foil of alloy with Al addition due to extreme brittleness was prepared by focused ion beam (FIB) method.

3. Results and discussion

The results of microstructure observations of as homogenized as well as solution treated (ST) alloys are presented in Fig. 1. After homogenization all the investigated alloys have typical dendrite grains which differ in orientation and size due to the heat transfer conditions during solidification. An example microstructure of the 3Al alloy is presented in Fig. 1a. The ST caused disappearance of dendrites and formation of the granular microstructure with grains in size from 100 up to 500 μm (Fig. 1b). High density network of micro-cracks resulting from ST is also visible on grain boundaries as well as inside the grains causing embrittlement of alloys (Fig. 1c). In the areas close to the edge of a sample, the aggregations of martensitic grains were observed, especially in alloy without Al (0Al). They were most probably formed, due to internal stresses generated during the sample preparation process. The presence of such aggregates allows to expect that this alloy will exhibit good pseudoelastic properties in external magnetic field, as was presented by Pieczyska et. al. [9] in case of NiFeGa magnetic shape memory alloy.

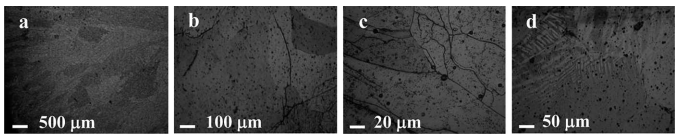

Fig. 1. LM microstructure images of a) as cast 3Al alloy and b), c), d) ST 0Al alloy

In Fig. 2 one can see XRD patterns of ST alloys recorded at room temperature; all ribbons show the same crystal structure of austenite with cubic $L2_1$ Heusler structure. However, only in the case of 0Al alloy the reflections corresponding to {111} supperlattice planes are visible. It suggests that addition of Al has an influence on the degree of the $L2_1$ phase order. Beside peaks corresponding to the $L2_1$ structure, the additional peaks at the 2 Theta position close to 45 and 52 degrees can also be distinguished. They are more pronounced in the case of alloys with the Al addition. These peaks may arise due to the pre-martenistic and/or martenistic transformation or they may originate from precipitation processes giving rise to precipitate phases (this would be in accordance with the thermal history of the samples and also the existence of stable and metastable phases originating from the quaternary Ni-Mn-Sn-Al system should not be underestimated). The formation of precipitates has been observed by Chen et al. [2], who reported it in martensite formed in similar Ni-Mn-Sn system with Al addition. Monoclinic martensite would also fit well with these positions. Thus, the detailed microstructure investigations are required for definite elucidation of these phenomena.

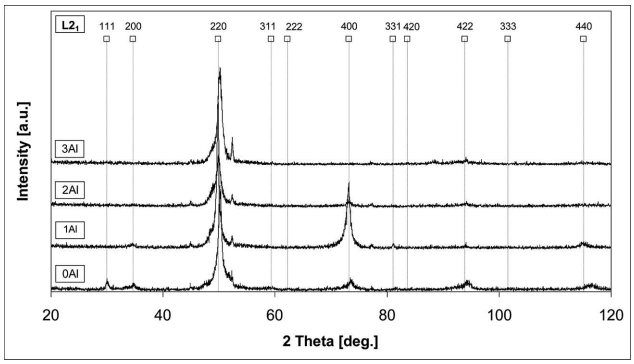

Fig. 2. Set of X-ray diffraction patterns of ST alloys with different aluminum content

Fig. 3 presents bright field (BF) microstructure image and the corresponding selected area diffraction pattern (SADP) of the 0Al alloy after ST. The SADP revealed that the Heusler ordered $L2_1$ parent phase with the [010] zone axis is present in the alloy at room temperature. Diffuse streaking of the two parallel Bragg diffraction superstructure spots along the <1 1 0> directions responsible for different ordered states is also observed at room temperature. Such a diffuse streaking is related to pre-martensitic transformation of intermediate phase. Its pattern comes from a multi-modulated area where modulations exist with different wave vectors and periodicities [10] and are consistent with a pretransitional state consisting

of a patchwork of "strain embryos" of a few nm in size as has been reported for Ni–Al and related alloy systems [11].

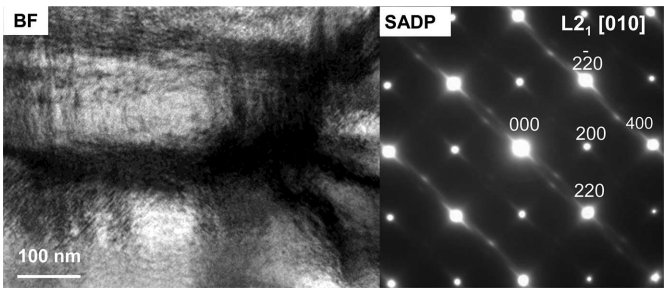

Fig. 3. Bright field (BF) microstructure and corresponding selected area diffraction pattern (SADP) of 0Al alloy after ST

Microstructure of alloys with Al addition is discussed based on the example of the 2Al alloy. At this point, it should be noted that samples with Al additions were more brittle than those without Al, and brittleness occurred to such an extent that it was impossible to prepare a thin foil by dimpling and ion milling, thus the FIB method was applied. Fig. 4 presents BF microstructure and the corresponding SADP of 2Al alloy after ST. The SADP indicates that this alloy at room temperature shows the ordered $L2_1$ structure with [011] zone axis, but also an extra reflections are visible in the SADP image. The origin of these reflections can be explained by precipitation process what was illustrated in the HAADF image shown as insert in Fig. 4. One can see a different contrast due to changes in chemical composition in form of very small bright spots. The chemical composition of the matrix and precipitates measured by EDS was as follows: (1) Ni-43, Mn-45, Sn-10, Al-2 and (2) Ni-44.7, Mn-40.6, Sn-10.4, Al-4.3, respectively. Above compositions corresponds to the following e/a ratios: e/a_{matrix} =7.91 and $e/a_{precipitate}$ =7.857. It is visible that mainly the differences occurs in relation to Al and Mn contents, however small differences in e/a ratios between precipitates and matrix has no significant influence on M_s temperature. So, it is worth noting that both changes of the degree of order of $L2_1$ parent phase as well as the precipitation process can occur as a result of Sn substitution by Al in $Ni_{44}Mn_{43.5}Al_xSn_{12.5-x}$ alloy system.

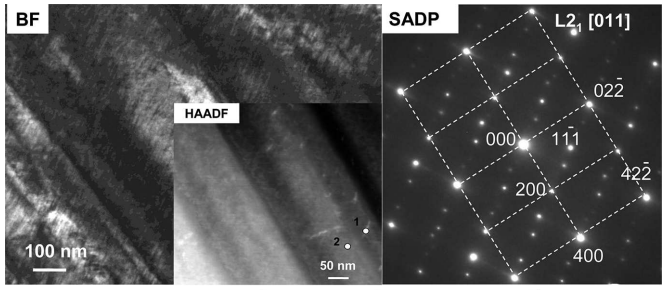

Fig. 4. BF (inset HAADF image) microstructure and corresponding and SADP of 2Al alloy after ST

The temperature range of martensitic and reverse transformations was determined by DSC measurements during cooling and heating cycles. Fig. 5 presents a set of DSC curves recorded during DSC cooling/heating cycles at the rate of 10°C/min. For all the investigated alloys the martensitic and reverse transformations occur below room temperature, however the addition of Al shifts them toward the higher temperature range. Also, an increase of the enthalpy of transformation was observed as the result of Al addition. Another characteristic phenomenon is related to broadening of peaks representing thermal effects, due to overlapping with both, the magnetic and pre-martensitic transformations. Thus, in order to plot a relationship between the Al addition (valence electron concentration of alloys, e/a) and data obtained from DSC measurements, a peak temperature was taken as representative for martensitic T_{pA-M} and T_{pM-A} reverse transformations, respectively. The hysteresis of transformations ΔT is the difference between T_{pA-M} and T_{pM-A}, and entropy changes were also calculated from T_{pA-M} and T_{pM-A} temperatures. The data obtained from DSC measurements for martensitic and reverse transformations are presented in Table 1.

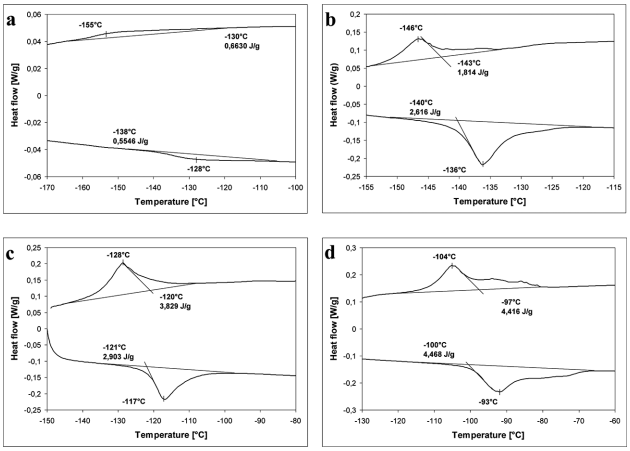

Fig. 5. Set of DSC curves recorded during cooling/heating cycles at 10°C/min for ST alloys a) 0Al, b) 1Al, c) 2Al and d) 3Al alloys

As mentioned before the martensitic transformation starts at higher temperature range when Al content increases. The entropy of transformation also increases, but the temperature hysteresis of transformation decreases. It is illustrated in Fig. 6, where the relationship between e/a and T_{pA-M} and ΔS_{pA-M} is plotted.

TABLE 1

Data obtained from DSC measurements characterizing a martensitic and reverse transformations in $Ni_{44}Mn_{43.5}Al_xSn_{12.5-x}$ (x= 0, 1, 2, 3 at. %) alloys

Alloy	e/a	Transformation temperatures [°C]			Entropy changes [J/gK]	
		T_{pA-M}	T_{pM-A}	ΔT	ΔS_{pA-M}	ΔS_{pA-M}
0Al	7.945	-155	-128	27	0.0056	0.0038
1Al	7.935	-146	-136	10	0.0143	0.0191
2Al	7.925	-128	-117	11	0.0264	0.0186
3Al	7.915	-104	-93	11	0.0261	0.0248

One can see that martensitic transformation start temperature increases with the decrease of e/a ratio and this is opposite to the reports by Krenke concerning Ni-Mn-X (X=Sn, In, Sb, Ga, Al) [12]. It means that substituting of Sn with Al leads to a decrease of the e/a ratio, yet at the same time the M_s temperature increases, which might be related to the reduction of

the unit cell volume induced by Al having a smaller atomic radii than Sn. The entropy of martensitic transformation also increases when e/a decreases. This phenomena is associated with a change of the degree of order of the $L2_1$ parent phase. For the lower values of entropy the parent $L2_1$ phase has high degree of order or even premartensitic transformation occurs as confirmed by TEM observations (Fig. 3). With an increase of Al content the increase of entropy occurs and a decrease of the degree of atomic order and precipitation were also observed and may also account for the overall effect on M_s. So, the substitution of Sn by Al in $Ni_{44}Mn_{43.5}Al_xSn_{12.5-x}$ (x= 0, 1, 2, 3 at. %) alloys causes an increase of martensitic transition start temperature but mechanism of this phenomena is very complex including change of the unit cell volume, change of the degree of atomic order of the parent austenite phase and precipitation.

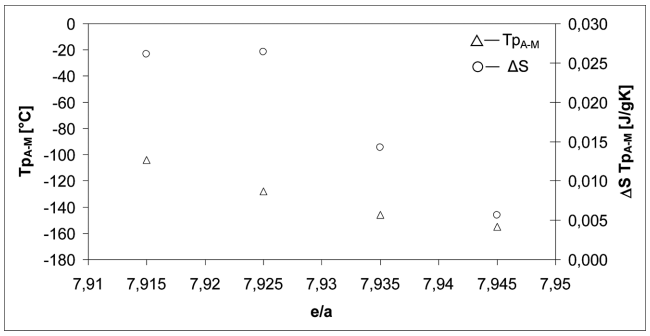

Fig. 6. Relationship between e/a of investigated alloys and T_{pA-M} and ΔS_{pA-M}

4. Conclusions

1. $Ni_{44}Mn_{43.5}Sn_{12.5-x}Al_x$ Heusler alloys are characterized by the granular microstructure with grains in size from 100 up to 500 μm and the network of high density of micro-cracks at the grains boundaries as well as inside the grains causing their brittleness.
2. Substitution of Sn with Al in $Ni_{44}Mn_{43.5}Sn_{12.5-x}Al_x$ Heusler alloys causes decrease of their e/a ratio and an increase both M_s temperature and entropy ΔS, and also a decrease of temperature hysteresis of martensitic and reverse transformations.
3. Increase of entropy of martensitic transformation as result of Al addition is associated with the change the degree of order of the $L2_1$ parent phase.
4. Precipitation process of very fine (few nanometers) precipitates was observed in alloys with the Al additions after solution treatment.

Acknowledgements

The results in presented paper partially have been obtained in frames of Project No. POIG.01.03.01-00-058/08.

REFERENCES

[1] W. Ito, X. Xu, R.Y. Umetsu, T. Kanomata, K. Ishida, R. Kainuma, Appl. Phys. Lett. **97**, 242512-1-3 (2010).
[2] J. Chen, Z. Han, B. Qian, P. Zhang, D. Wang, Y. Du, J. Magn. Magn. Mater. **323**, 248-251 (2011).
[3] T. Krenke, X. Moya, S. Aksoy, M. Acet, P. Entel, Ll. Manosa, A. Planes, Y. Elerman, A. Yucel, E.F. Wassermann, J. Magn. Magn. Mater. **310**, 2788-2789 (2007).
[4] X. Moya, Ll. Manosa, A. Planes, T. Krenke, M. Acet, E.F. Wassermann, Mater. Sci. Eng. **A 438-440**, 911-915 (2006).
[5] L. Chen, F.X. Hu, J. Wang, J.L. Zhao, J.R. Sun, B.G. Shen, J.H. Yin, L.Q. Pan, J. Phys. D: Appl. Phys. **44**, 085002 (2011).
[6] W. Ito, M. Nagasako, R.Y. Umetsu, R. Kainuma, T. Kanomata, K. Ishida, Appl. Phys. Lett. **93**, 232503 (2008).
[7] Z.G. Wei, R. Sandstrom, Scripta Mater. **11**, 1727-1732 (1997).
[8] J. Dubowik, I. Gościańska, A. Szlaferek, Y.V. Kudryavtsev, Mater. Sci. Poland **25**, 583-598 (2007).
[9] E. Pieczyska, J. Dutkiewicz, F. Masdeu, J. Luckner, R. Maciak, Archives of Metallurgy and Materials **56**, 2, 401-408 (2011).
[10] L. Liu, S. Fuc, Z. Liu, G. Wu, X. Suna, J. Li, Journal of Alloys and Compounds **425** 176-180 (2006).
[11] D. Schryvers, L.E. Tanner, Ultramicroscopy **32**, 241 (1990).
[12] T. Krenke, M. Acet, E.F. Wassermann, X. Moya, L. Manosa, A. Planes, Phys. Rev. **B 73** (2006).

Received: 20 January 2013.